1 **Comparison of ~~slant open-path~~ flux gradient and ~~static closed~~ chamber techniques to**

2 **measure soil N_2O emissions**

3 Mei Bai[1,*], Helen Suter[1], Shu Kee Lam[1], Thomas K. Flesch[2], Deli Chen[1]

4 [1]Faculty of Veterinary and Agricultural Sciences, The University of Melbourne, Parkville, VIC

5 3010, Australia

6 [2]Department of Earth and Atmospheric Sciences, University of Alberta, Edmonton, AB ~~T6G~~

7 ~~2R3~~T6E 2H4, Canada

8 *Correspondence to*: Mei Bai (mei.bai@unimelb.edu.au)

9

10 **Abstract**

11 Improving ~~the~~ direct field measurement techniques to quantify gases emissions from ~~the large~~

12 ~~agriculture farm~~cropped agricultural fields is challenging. We compared nitrous oxide (N_2O)

13 emissions measured with static closed chambers to those from a newly developed

14 ~~micrometeorological~~aerodynamic flux gradient (FG) approach. Measurements were made at a

15 vegetable farm following chicken manure application. The FG calculations were made with a

16 single open-path Fourier transform infrared (OP-FTIR) spectrometer (height of 1.45 m)

17 deployed in a slant-path configuration: sequentially aimed at retro reflectors at heights of 0.8

18 and 1.8 m above ground. Hourly emissions were measured with the FG technique, but once a

19 day between 10:00 and 13:00 with chambers. We compared the concurrent emission ratios

20 (FG/Chambers) between these two techniques, and found N_2O emission rates from celery crop

21 farm measured at mid-day by FG were statistically higher (1.~~4~~22−1.40 times) than those from

22 the chambers measured at the same time. Our results suggest the OP-FTIR slant-path FG

23 configuration worked well in this study: it was sufficiently sensitive to detect the N_2O gradients

24 over our site, giving high temporal resolution N_2O emissions corresponding to a large

25 measurement footprint.

26

1 Introduction

The accurate measurement of soil nitrous oxide (N_2O) emissions from agricultural land is challenging. Chambers are commonly used for these measurements (Hutchinson and Mosier, 1981), and chamber based observations are widely used to calculate greenhouse gas inventories (Dalal et al., 2008). The principle behind the most common type of chamber measurement (static, or non-steady state) is to create a sealed control volume over the soil surface, such that by monitoring the gas concentration change during the chamber deployment, one can calculate the surface emission rate (Denmead, 2008). One of the advantages of chambers is that they can be employed at relatively low cost, with simplicity and easy field operation (de Klein et al., 2001). However, chambers have a fundamental limitation – the control volume inevitably perturbs the soil-atmosphere interface (e.g., temperature, pressure), which has the potential to modify the ambient soil emission rate (Denmead, 1979). Moreover, manually operated static chambers are not well-suited to measure temporal variations in emissions (Denmead et al., 2008; Jones et al., 2011). These weaknessesThe temporal variation issue can be addressed by alternative approaches, e.g. a dynamic measurement with automated-chamber opening and closing by pneumatic actuators (Yao et al., 2009) and can be run for many months. However, in many situations the most important disadvantage of chambers is their small surface measurement footprint. With a surface enclosure typically less than 1 m², and the likelihood that soil emissions vary dramatically at length scales greater than 1 m (Denmead, 2008; Griffith

and Galle, 2000; Turner et al., 2008), many replications are needed to adequately quantify the emissions from an agricultural field (Christensen et al., 1996; Denmead, 1995).

Micrometeorological measurements avoid some of the problems associated with chamber methods (Christensen et al., 1996; Denmead et al., 2010; Li et al., 2008; Pattey et al., 2006). These techniques are based on concentration and windflow measurements made in the free air above the surface, and they do not perturb the surface environment. They also measure emissions over footprints much larger than those from chambers (Hargreaves et al., 1996). The aerodynamic flux gradient (FG) technique is a well-used micrometeorological method, where the vertical flux of gas is inferred from a height gradient in concentration (multiplied by an estimate of the gasturbulent diffusivity). When measured above a large and homogeneous surface, this atmospheric flux is assumed equal to the underlying surface emission or absorption rate. In this study we used a recently developed modification of the technique. Rather than vertically separated point concentrations, we used a slant-path configuration based on vertically separated long line-averaged measurements (Flesch et al., 2016; Wilson and Flesch, 2016). A single open-path Fourier transform infrared (OP-FTIR) concentration sensor with motorized aiming gives the gas concentrations along the two paths, from which we can calculate the surface emission/deposition rate.

In this study we conducted a set of N_2O emission measurements from a vegetable farm following manure application. Measurements were made with both static chambers and the slant-path FG approach. Our objective was to 1) demonstrate the newly developed slant-path FG method at a vegetable farm; and 2) compare the emission rates measured by the static chamber and FG techniques.

2 Materials and methods

2.1 Experimental site

This study was conducted at an intensive vegetable farm in Clyde, Victoria, Australia (38.1° S, 145.3° E). The site consisted of two adjacent fields of 5.4 ha (Site 1) and 3.1 ha (Site 2). These sites differ only in the addition of a fertilizer amendment at Site 2. A celery crop at the 4-5 leaf stage was transplanted to these two sites on 27 Febuary 2014 (Fig. 1). Chicken manure (4.3% N, NH_4^+-N: 4633 mg kg^{-1}, NO_3-N: 313 mg kg^{-1}) was applied at rate of 8.2 tonne ha^{-1} at both sites on 28 March. Fertiliser Cal-Gran (a blend of calcium ammonium nitrate and ammonium sulphate, total 23.9% N) was also applied at both sites at rate of 200 kg ha^{-1} on 15 April. Emission measurements began just prior to manure application and ended on 6 May 2014. The terrain was open and flat with sandy loam topsoils. Prevailing winds were southeast or northwest during this period. The average daily minimum and maximum temperature ~~was~~were 6 and 33°C, respectively. The total precipitation (including rainfall and irrigation) during the measurement period was 186 mm.

Figure 1

2.2 Methodologies

2.2.1 Static chamber

Four static chambers ($50 \times 50 \times 25$ cm) were located at each site (Fig. 1). The metal base for each chamber was placed into the soil to a depth of 8 cm prior to the experiment, and remained in place through the study. The chamber was made of plexiglass with a built in ventilation system. Reflective aluminium foil was attached inside the lid to minimize changes in ambient pressure and temperature after the chamber was placed onto the base. A thermocouple Tinytag Transit 2 (TG-4080 temperature loggers, West Sussex, UK) was placed on the soil surface inside the chamber to monitor the headspace air temperature. Gas samples (20 mL) were

102 collected into evacuated 12 mL vials (Exetainer®, Labco Ltd., Ceredigion, UK) at 0, 30 and

103 60 minutes after chamber placement and analysed at an off-site laboratory by gas

104 chromatography (GC) (Agilent 7890A, Wilmington, USA). The sensitivity of GC for N_2O

105 concentration was 0.01 ppm. Gas samples were collected daily between 10:00 and 13:00 from

106 29 March to 7 April and on 9, 11 and 16 April. The N_2O flux was calculated as (Ruser et al.,

107 1998) (Eq. 1):

108 $Q_{chamber} = \text{~~κ~~}\underline{K_{N2O}}\ (273/T)\ (V/A)\ dC/dt$ (1)

109 where $Q_{chamber}$ is the gas flux (µg N_2O−N m^{-2} h^{-1}~~), κ~~)$;$ $\underline{K_{N2O}}$ is ~~a density factor for N_2O gas,~~ 1.25

110 (µg N µL^{-1}~~,~~) according to the ideal gas law, where $\underline{K_{N2O} = P\ m/R\ T_0}$, and P is air pressure (at

111 1 atm), m is molecular mass (28 g mol^{-1}), R is gas constant (0.0821 L atm K^{-1} mol^{-1}), and T_0 is

112 273 K; T is the air temperature within the chamber (K~~,~~); V is the total volume of headspace

113 (L~~,~~); A is a surface area inside the chamber (m^2~~,~~); and dC/dt is the rate of change in

114 ~~concentration~~mole fraction of N_2O in the chamber (µL L^{-1} h^{-1}~~.~~) determined by linear

115 regression model. The N_2O mole fraction is provide by GC, in ppm.

116

2.2.2 Flux gradient

118 The basic principle of the FG method has been well-described (Judd et al., 1999; Laubach and

119 Kelliher, 2004; Webb et al., 1980). We followed a modification described in Flesch et al.

120 (2016), in which an open-path sensor was used to measure the concentration difference (ΔC_L)

121 between two vertically offset slant-paths. The open-path sensor measures gas concentration

122 between the sensor and a distant retro reflector. The concentration difference ΔC_L is calculated

123 by sequentially aiming the sensor at high and low retro reflectors ~~(Eqs. 2, 3):~~. Flesch et al.

124 (2016) showed that the conventional FG eqution can be transformed into Eqs. 2, 3:

125 $Q_{FG} = (k_v \rho_a\ u_*/S_c)(M_s/M_a)\ *\kappa\ *\Delta C_L$ (2)

126 $$\kappa = l_{PATH} / \int_{x1}^{x2} [\ln(z_{p2}/z_{p1}) - \varphi(z_{p2}/L) + \varphi(z_{p1}/L)]dx \qquad (3)$$

127 where Q_{FG} is the gas flux (g m^{-2} s^{-1}), k_v is von Karman's constant (0.4), ρ_a is dry air density (g

128 m^{-3}), u_* is friction velocity (m s^{-1}), S_c is the turbulent Schmidt number (0.64), M_s and M_a are

129 the molar mass of N$_2$O (44 g mol^{-1}) and dry air (29 g mol^{-1}), respectively, ΔC_L (ppb) is the

130 difference in the line-average volumetric mixing ratio of the gas (relative to dry air) from the

131 lower (z_{p1}) and upper (z_{p2}) paths (m, relative to celery beds surface), κ is proportional to the

132 height integral of the gas diffusivity along the FTIR path pair, l_{PATH} is the sensor-retro reflector

133 path length (m, equal for the two paths), L is atmospheric Obukhov stability length (m). Path

134 heights (z_{p1} and z_{p2}) along the path length are given by a 5th-order polynomial fit of height vs.

135 distance from the OP-FTIR spectrometer (path heights were measured in the field at 5 m

136 intervals). We used the stability correction factor φ from Flesch et al. (2016).

137

138 An estimate of the uncertainty in Q_{FG} (δ_{QFG}) was calculated as the sum in quadrature of the

139 relative uncertainties in S_c, ΔC_L and κ according to the formula described in Flesch et al. (2016).

140 Q_{FG} values were not calculated when $u_* < 0.05$ m s^{-1}.

141

142 The FG calculations relied on open-path concentrations measured with a robust Bruker OP-

143 FTIR spectrometer (Matrix-M IRcube, Bruker Optics, Ettlingen, Germany) and two retro

144 reflectors located 80 m from the spectrometer (PLX Industries, New York, USA). Briefly, the

145 OP-FTIR system measures multiple gas concentrations (N$_2$O, CH$_4$, NH$_3$, CO$_2$, CO and water

146 vapour) with high precision (N$_2$O < 0.3 ppb, CH$_4$ < 2 ppb, NH$_3$, 0.4ppb, CO$_2$, 1 ppm, CO, 0.1

147 ppb, and water vapour < 5%) (Griffith, 1996; Griffith et al., 2008; Griffith et al., 2012). More

148 details on the OP-FTIR system can be found in Bai (2010). The spectrometer was mounted at

149 a height of 1.45 m above ground. A motorized mounting head sequentially aimed the

spectrometer to the retro reflectors at 0.8 and 1.8 m above ground. Line-averaged N_2O

concentrations with an averaging time of 2.5-min were measured. Background N_2O

concentrations were measured prior to manure application in order to assess measurement

precision. A sequence of obsevations were averaged, the standard deviation of the mean was

retrieved and the precision of N_2O concentration measurements (less than 0.3 ppb) was

determined according to Bai (2010). The OP-FTIR measurements were made continuously

from 25 March until 16 April, and thereafter measurements were made for three days

(continuously) per week until 6 May.

A weather station coupled with a three-dimensional sonic anemometer (CSAT3, Campbell

Scientific, Logan, UT, USA) was established at a height of 3.0 m above ground, 50 m east of

Site 2. Fifteen-min average climatic data including ambient temperature, pressure and wind

statistics were recorded by a data logger (CR23X, Campbell Scientific, Logan, UT, USA) at a

frequency of 10 Hz. Atmospheric stability parameters of friction velocity (u_*), surface

roughness (z_0) and Obukhov stability length (L) were calculated from the ultrasonic

anemometer data. We used a data filtering procedure to remove error-prone observations in the

FG calculation according to Flesch et al. (2014).

To

The FG flux measurements correspond to surface emissions within a flux "footprint". The

footprint generally extends upwind of the concentration sensors, but its spatial size varies with

wind conditions. A concern of this study is that the FG footprint extends beyond our plots, and

the calculated emission rates are "contaminated" by emissions occurring outside the plot. This

possibility was investigated by modelling the FG footprint for our smaller Site 2, where the

contamination concerns are greater. The WindTrax dispersion software

(thunderbeachscientific.com) was used to simulate the OP-FTIR slant-path setup, and calculate

175 the fraction of the FG measured flux occurring within the Site 2 plot. We looked at the wind

176 direction that results in a short fetch (NE), and looked at different atmospheric stability

177 conditions and roughness lengths. The results for $z_0 = 0.1$ m (representative of the plot) are

178 shown in Figure 2. We concluded that during stable night-time conditions the FG emission

179 calculations for Site 2 maybe contaminated by up to 40% by outside fluxes. This may result in

180 either over- or under-estimation of Site 2 emissions depending on the emission rate outside the

181 plot. In unstable daytime conditions the contamination potential falls to 0−10%. Contamination

182 at Site 1 will not be as serious due to the larger fetches.

183

184 The main objective of our study is to compare ~~the two measurement techniques we~~chamber

185 and FG emission estimates. We looked at periods with concurrent measurements from ~~FG and~~

186 the ~~chambers~~two techniques, and hourly flux ratios of $Q_{FG}/Q_{chamber}$ measured between 10:00

187 and 13:00 are compared. Because the comparison took place during the day when conditions

188 were generally unstable, the FG contamination potential is low (and will be ignored). The

189 contamination potential does highlight a concern with micrometeorological measurements, that

190 a large measurement footprint may extend outside the study area and result in measurement

191 errors.

192 Figure 2

193

194 **3 Results and discussion**

195 **3.1 Daily N$_2$O flux**

196 The FG measurements gave high temporal resolution of fluxes and this provides an opportunity

197 to study the pattern of N$_2$O emissions in detail. Here we only describe the temporal flux

198 measurements from Site 1.

199

3.1.1 The ~~FG~~flux gradient fluxes

Hourly N_2O fluxes showed large temporal variation during the experimental period in response to fertilisation. There was a rapid increase in N_2O emission from a background level of 0.6 mg $N_2O−N$ m^{-2} h^{-1} before manure application to a peak of 158.0 mg $N_2O−N$ m^{-2} h^{-1} within 24 h after application, which could be attributed to both nitrification and denitrification. After the peak, several spikes between 16−17 April were also observed associated with fertilizer application, followed by a decline in emissions to an average of 2.5 mg $N_2O−N$ m^{-2} h^{-1} (Fig. ~~2A~~3A). One of the conclusions we draw from Figure ~~2B~~3B is that the slant path FG system is sensitive enough to measure the N_2O fluxes that accompanied fertilisation at our site, i.e., the measurement uncertainty as represented by 1-σ is generally well below the flux magnitude.

In addition to the long-term pattern of decreasing emissions after manure application, we observed a diurnal pattern where maximum emission tended to occur in the late afternoon (16:00) (Fig. ~~2B~~3B). We believe this is related to the time of maximum soil surface temperature, which occurs after the peak air temperature (Christensen et al., 1996; Wang et al., 2013). A strong diurnal emission pattern implies that once-a-day snapshot emission measurements (e.g., chambers) would almost certainly give a biased estimate of the daily average emission rate. We also noticed occasional high emissions at night, which was closely related to precipitation events. Negative N_2O fluxes calculated from the FG measurements most likely represent instrument noise, as the flux magnitudes were below the detectable limit of our OP-FTIR system, i.e~~.g~~., the uncertainty represented by the 1-σ error bars in Fig. ~~2~~3 span zero. Figure ~~2~~3

3.1.2 Chamber fluxes

9

Nitrous oxide fluxes from the static chambers (once-a-day snapshots) were in general agreement with the FG measurements in terms of the long-term ~~pattern~~background exchange patterns (Fig. ~~2~~3): hourly fluxes rose from a background level of 1.12 mg N_2O-N m^{-2} h^{-1} (before manure application, data is not shown), reached a spike of 3.48 mg N_2O-N m^{-2} h^{-1} 48 hours after manure application, then dropped to a minimum of 1.02 mg N_2O-N m^{-2} h^{-1} on 5 April. A maximum emission peak of 3.55 mg N_2O-N m^{-2} h^{-1} was measured on 16 April and was most likely related to fertilizer application.

3.2 Comparison of the two ~~emission~~measurement techniques

We selected the concurrent measurements from FG and the chambers and a total of 23 comparison pairs were obtained during the study period (note that each chamber observation is an average from four replicate chambers). We calculated the ratio $Q_{FG}/Q_{chamber}$ of these concurrent pairs.

The $Q_{FG}/Q_{chamber}$ ratio showed large variation, with values ranging between 0.4 and 4.9. The $Q_{FG}/Q_{chamber}$ data follows a non-normal distribution. To better interpret these data we log-transformed the ratios (Abdi et al., 2015). The average of the natural logarithm of the ratio, converted back to the ratio units, gives the geometric mean (the process was duplicated to calculate the confidence interval $\alpha = 0.9$). The geometric mean of $Q_{FG}/Q_{chamber}$ was 1.40, with a confidence interval ranging from 1.15 to 1.69. This means that on average the FG measured fluxes were 40% higher than those from the chambers, and this difference was statistically significant.

Differences between chamber and micrometeorological measurements have been previously noted. Some studies have reported that micrometeorological techniques gave emission rates

249   that were 50−60% of those from chambers (Christensen et al., 1996; Neftel et al., 2010). In

250   contrast, Wang et al. (2013) reported N_2O emissions measured by chambers were 17−20%

251   lower than from the eddy covariance micrometeorological technique, and Norman et al. (1997)

252   reported that chamber measurements were 30% lower than micrometeorological

253   measurements. Sommer et al. (2004) found static vented chambers underestimated N_2O

254   emissions from manure piles by 12−22% compared to mass balance measurements.

255

256   Discrepancies between FG and chamber fluxes could be due to very different measurement

257   footprints. Large spatial variability is a characteristic of soil N_2O emissions. For example,

258   Turner et al. (2008) reported N_2O emissions varied from 30 to 800 ng $N_2O−N$ m^{-2} s^{-1} over an

259   irrigated dairy pasture (8,100 m^2). This high variability, together with the substantial difference

260   in measurement footprint size (chambers < 1 m^2 vs FG > 1000 m^2) will likely result in

261   differences between the two techniques because the chambers are not capable of accounting

262   for this variability, unless many chambers are used, whilst the FG method can. If this explains

263   the difference between the two techniques, then discrepancies between chambers and

264   micrometeorological techniques should be site dependent, i.e., dependent on the degree of

265   spatial variability in emissions at each site.

266

267   Several researchers have reported that chamber flux calculation procedures introduced large

268   uncertainty in N_2O emissions (Levy et al., 2011; Venterea et al., 2010). In particular, using

269   linear regression to determine the rate of change dC/dt in Eq. (1) can lead to an underestimate

270   of emissions (Anthony et al., 1995; Matthias et al., 1978). Venterea (2013) concluded that the

271   typical calculations used for non-steady state chambers underestimated N_2O emissions by

272   20−50%. ~~Our results are in line with this conclusion.~~To examine the potential bias in N_2O

273   emissions when dC/dt is estimated with a linear regression model, we also calculated the results

274   using a non-linear monomolecular model (Bolker, 2007). The monomolecular model is one of

275   the simplest saturating functions and follows (Eq. 4):

276   $C_{N2O} = a_0 + a_1 (1 - \exp(-a_2/a_1 * t))$ (4)

277   where C_{N2O} is the mole fraction of N_2O, a_0 is the intercept corresponding to the N_2O mole

278   fraction at time $t = 0$, a_1 is the horizontal asymptote at $t = +\infty$, a_2 is the slope (dC/dt) at $t = 0$,

279   and t is time after chamber placement (h).

280

281   Chamber fluxes calculated using the non-linear dC/dt ($Q_{chamber-non-linear}$) were 1.15 times higher

282   than $Q_{chamber}$ estimated using linear regression. Comparing the concurrent fluxes of Q_{FG} and

283   $Q_{chamber-non-linear}$, we found the geometric mean of $Q_{FG}/Q_{chamber-non-linear}$ to be 1.22 (confidence

284   interval of 0.99 to 1.49). Using 10,000 bootstrap re-samples (Efron and Tibshirani, 1994), we

285   computed 10,000 potential mean fluxes from the non-linear model, of which 9540 of the means

286   were greater than 1, and 460 were lower than 1. This result suggests the use of the non-linear

287   dC/dt calculation has resulted in better agreement with the FG estimates.

288

289   While there is a long and successful history of FG applications, there are still questions about

290   its implementation. The value of the turbulent Schmidt number (S_c) in Eq. (2) is debated (Flesch

291   et al., 2002). ~~In addition, concerns about FG arise if the fetch (upwind distance from the~~

292   ~~concentration measurement to the source edge) is not large. In our case the ratio of z_1 (the~~

293   ~~maximum height of the OP-FTIR measurement path, 1.8 m) to the upwind fetch (minimum of~~

294   ~~90–68 m for Sites 1 and 2, respectively) was < 1:35. This is considered to be sufficient in most~~

295   ~~conditions, but during stable night-time conditions the fetch may not have been large enough~~

296   ~~to satisfy the FG assumption of a constant flux layer (Flesch et al., 2016). In this case the FG~~

297   ~~measurements would have been contaminated by emissions occurring upwind of our sites.~~

298   There is also a concern regarding the accuracy of FG during light winds. In our study the light

299 wind data ($0.05-0.15$ m s^{-1}) accounted for 24% of the measurement periods. We found the FG

300 uncertainty (δ_{QFG}/Q_{FG}) increased from 0.41 to 1.25 when the friction velocity (u_*) dropped from

301 0.15 to 0.05 m s^{-1}. However, we note that in this study the periods in which we compared FG

302 and chamber measurements were not light wind periods.

303

304 4 Conclusions

305 Our results showed that ~~FG and static chamber measurements of~~ soil N$_2$O emissions measured

306 by FG and static chambers (linear dC/dt) were statistically different, with fluxes from FG being

307 on average 40% higher. Using a non-linear calculation of dC/dt in the chambers decreased the

308 disagreement to 22%. Given the likelihood of large spatial variability in N$_2$O emissions, and

309 the vastly different measurement footprints of the two methods, it is not surprising the two

310 techniques give different results. It is difficult to conclude that one technique or the other is

311 biased based on this experiment alone. However, the relationship we observed, together with

312 other reports on the biases created by chamber calculation procedures, supports an

313 interpretation that our FG emission calculations were accurate and in this instance the chamber

314 measurements were biased too low.

315

316 The OP-FTIR flux gradient system used here showed the capability for real-time emission

317 measurements over a large spatial footprint with no surface interference. Furthermore, being

318 free from pumps and tubing, the open-path FG system would be particularly advantageous for

319 measuring multiple gas emissions including "sticky" gases like NH$_3$.

320

321 5 Author contribution

DC, HS, SKL, MB and TF designed the experiments and MB and SKL carried them out. TF

and MB developed the techniques. MB prepared the manuscript with contributions from all

co-authors.

6 Competing interests

The authors declare that they have no conflict of interest.

7 Acknowledgments

References

Abdi, D., Cade-Menun, B.J., Ziadi, N., Parent, L.-É., 2015. Compositional statistical analysis of soil ^{31}P-NMR forms. Geoderma. 257–258, 40-47.

Anthony, W.H., Hutchinson, G.L., Livingston, G.P., 1995. Chamber measurement of soil-atmosphere gas exchange: Linear vs. diffusion-based flux models. Soil Sci. Soc. Am. J. 59, 1308-1310.

Bai, M., 2010. Methane emissions from livestock measured by novel spectroscopic techniques, School of Chemistry. University of Wollongong, p. 303.

Bolker, B., 2007. Ecological Models and Data in R. Princeton University Press, The United States of America.

Christensen, S., Ambus, P., Arah, J.R.M., Clayton, H., Galle, B., Griffith, D.W.T., Hargreaves, K.J., Klemedtsson, L., Lind, A.M., Maag, M., Scott, A., Skiba, U., Smith, K.A.,

Welling, M., Wienhold, F.G., 1996. Nitrous oxide emission from an agricultural field: comparison between measurements by flux chamber and micrometerological techniques. Atmos. Environ. 30, 4183.

Dalal, R.C., Allen, D.E., Livesley, S.J., Richards, G., 2008. Magnitude and biophysical regulators of methane emission and consumption in the Australian agricultural, forest, and submerged landscapes: a review. Plant Soil. 309, 43-76.

de Klein, C.A.M., Sherlock, R.R., Cameron, K.C., van der Weerden, T.J., 2001. Nitrous oxide emissions from agricultural soils in New Zealand—A review of current knowledge and directions for future research. J. Roy. Soc. New Zeal. 31, 543-574.

Denmead, O.T., 1979. Chamber systems for measuring nitrous oxide emission from soils in the field. Soil Sci. Soc. Am. J. 43, 89-95.

Denmead, O.T., 1995. Novel meteorological methods for measuing trace gas fluxes. Philos. T. R. Soc. A. 351, 383-396.

Denmead, O.T., 2008. Approaches to measuring fluxes of methane and nitrous oxide between landscapes and the atmosphere. Plant and Soil. 309, 5-24.

Denmead, O.T., Chen, D., Griffith, D.W.T., Loh, Z.M., Bai, M., Naylor, T., 2008. Emissions of the indirect greenhouse gases NH_3 and NO_x from Australian beef cattle feedlots. Aust. J. Exp. Agr. 48, 213-218.

Denmead, O.T., Macdonald, B.C.T., Bryant, G., Naylor, T., Wilson, S., Griffith, D.W.T., Wang, W.J., Salter, B., White, I., Moody, P.W., 2010. Emissions of methane and nitrous oxide from Australian sugarcane soils. Agric. Forest Meteorol. 150, 748-756.

Efron, B., Tibshirani, R.J., 1994. An intruduction to bookstrap. Chapman&Hall/CRC, Boca Raton, London, New York, Washington, D.C.

Flesch, K.T., Baron, V., Wilson, J., Griffith, D.W.T., Basarab, J., Carlson, P., 2016. Agricultural gas emissions during the spring thaw: Applying a new measuremnt technique. Agric. Forest Meteorol. 221, 111-121.

Flesch, T.K., McGinn, S.M., Chen, D.L., Wilson, J.D., Desjardins, R.L., 2014. Data filtering for inverse dispersion emission calculations. Agric. Forest Meteorol. 198-199, 1-6.

Flesch, T.K., Prueger, J.H., Hatfield, J.L., 2002. Turbulent Schmidt number from a tracer experiment. J. Appl. Meteorol. 111, 299-307.

Griffith, D.W.T., 1996. Synthetic calibration and quantitative analysis of gas-phase FT-IR spectra. Appl. Spectrosc. 50, 59-70.

Griffith, D.W.T., Bryant, G.R., Hsu, D., Reisinger, A.R., 2008. Methane emissions from free-ranging cattle: comparison of tracer and integrated horizontal flux techniques. J. Environ. Qual. 37, 582-591.

Griffith, D.W.T., Deutscher, N.M., Caldow, C., Kettlewell, G., Riggenbach, M., Hammer, S., 2012. A Fourier transform infrared trace gas and isotope analyser for atmospheric applications. Atmos. Meas. Tech. 5, 2481-2498.

389   Griffith, D.W.T., Galle, B., 2000. Flux measurements of NH_3, N_2O and CO_2 using dual beam
390   FTIR spectroscopy and the flux gradient technique. Atmos. Environ. 34, 1087-1098.

391   Hargreaves, K.J., Wienhold, F.G., Klemedtsson, L., Arah, J.R.M., Beverland, I.J., Fowler, D.,
392   Galle, B., Griffith, D.W.T., Skiba, U., Smith, K.A., Welling, M., Harrris, G.W., 1996.
393   Measurement of nitrous oxide from Agricultural land using micrometeorological methods.
394   Atmos. Environ. 30, 1563-1571.

395   Hutchinson, G.L., Mosier, A.R., 1981. Improved soil cover method for field measurement of
396   nitrous oxide fluxes. Soil Sci. Soc. Am. J. 45, 311-316.

397   Jones, S.K., Famulari, D., Di Marco, C.F., Nemitz, E., Skiba, U.M., Rees, R.M., Sutton,
398   M.A., 2011. Nitrous oxide emissions from managed grassland: a comparison of eddy
399   covariance and static chamber measurements. Atmos. Meas. Tech. 4, 2179-2194.

400   Judd, M.J., Kellier, F.M., Ulyatt, M.J., Lassey, K.R., Tate, K.R., Shelton, D., Harvey, M.J.,
401   Walker, C.F., 1999. Net methane emissions from grazing sheep. Global Change Biol. 5, 647-
402   657.

403   Laubach, J., Kelliher, F.M., 2004. Measuring methane emission rates of a dairy cow herd by
404   two micrometeorological techniques. Agric. Forest Meteorol. 125, 279-303.

405   Levy, P.E., Gray, A., Leeson, S.R., Gaiawyn, J., Kelly, M.P.C., Cooper, M.D.A., Dinsmore,
406   K.J., Jones, S.K., Sheppard, L.J., 2011. Quantification of uncertainty in trace gas fluxes
407   measured by the static chamber method. Eur. J. Soil Sci. 62, 811-821.

408   Li, J., Tong, X., Yu, Q., Dong, Y., Peng, C., 2008. Micrometeorological measurements of
409   nitrous oxide exchange above a cropland. Atmos. Environ. 42, 6992-7001.

410   Matthias, A.D., Yarger, D.N., Weinback, R.S., 1978. A numerical evaluation of chamber
411   methods for determining gas fluxes. Geophys. Res. Lett. 5, 765-768.

412   Neftel, A., Ammanna, C., Fischer, C., Spirig, C., Conen, F., Emmenegger, L., Tuzson, B.,
413   Wahlen, S., 2010. N_2O exchange over managed grassland: Application of a quantum cascade
414   laser spectrometer for micrometeorological flux measurements. Agric. Forest Meteorol. 150,
415   775-785.

416   Norman, J.M., Kucharik, C.J., Gower, S.T., Baldocchi, D.D., Crill, P.M., Rayment, M.,
417   Savage, K., Striegl, R.G., 1997. A comparison of six methods for measuring soil-surface
418   carbon dioxide fluxes. J. Geophys. Res. 102, 28771-28777.

419   Pattey, E., Strachan, I.B., Desjardins, R.L., Edwards, G.C., Dow, D., MacPherson, J.I., 2006.
420   Application of a tunable diode laser to the measurement of CH_4 and N_2O fluxes from field to
421   landscape scale using several micrometeorological techniques. Agric. Forest Meteorol. 136,
422   222-236.

423   Ruser, R., Flessa, H., Schilling, R., Steindl, H., Beese, F., 1998. Soil compaction and
424   fertilization effects on nitrous oxide and methane fluxes in potato fields. Soil Sci. Soc. Am. J.
425   62, 1587-1595.

426   Sommer, S.G., McGinn, S.M., Hao, X., Larney, F.J., 2004. Techniques for measuring gas
427   emissions from a composting stock pile of cattle manure. Atmos. Environ. 38, 4643-4652.

428   Turner, D.A., Chen, D., Galbally, I.E., Leuning, R., Edis, R.B., Li, Y., Kelly, K., Phillips, F.,
429   2008. Spatial variability of nitrous oxide emissions from an Australian irrigated dairy pasture.
430   Plant and Soil. 309, 77-88.

431   Venterea, R.T., 2013. Theoretical comparison of advanced methods for calculating nitrous
432   oxide fluxes using non-steady state chambers. Soil Sci. Soc. Am. J. 77, 709-720.

433   Venterea, R.T., Dolan, M., Ochsner, T.E., 2010. Urea decreases nitrous oxide emissions
434   compared with anhydrous ammonia in a Minnesota corn cropping system. Soil Sci. Soc. Am.
435   J. 74, 407-418.

436   Wang, K., Zheng, X., Pihlatie, M., Vesala, T., Liu, C., Haapanala, S., Mammarella, I.,
437   Rannik, Ü., Liu, H., 2013. Comparison between static chamber and tunable diode laser-based
438   eddy covariance techniques for measuring nitrous oxide fluxes from a cotton field. Agric.
439   Forest Meteorol. 171–172, 9-19.

440   Webb, E.K., Pearman, G.I., Leuning, R., 1980. Correction of flux measurements for
441   chemistry effects due to heat and water vapour transfer. Quart. J. R. Meteorol. Soc. 106, 85-
442   100.

443   Wilson, J.D., Flesch, T.K., 2016. Generalized flux-gradient technique pairing line-average
444   concentrations on vertically separated paths. Agric. Forest Meteorol. 220, 170-176.

445   Yao, Z., Zheng, X., Xie, B., Liu, C., Mei, B., Dong, H., Butterbach-Bahl, K., Zhu, J., 2009.
446   Comparison of manual and automated chambers for field measurements of N_2O, CH_4, CO_2
447   fluxes from cultivated land. Atmos. Environ. 43, 1888-1896.

448

449   **Figures**

450   Figure 1

451

452

453
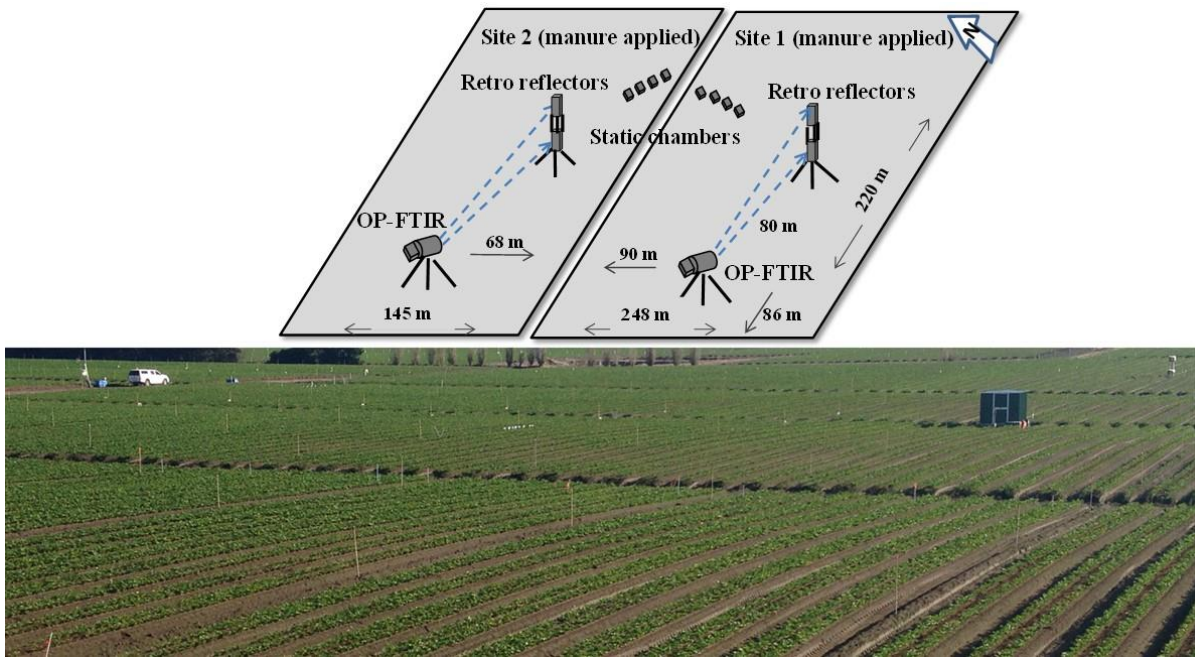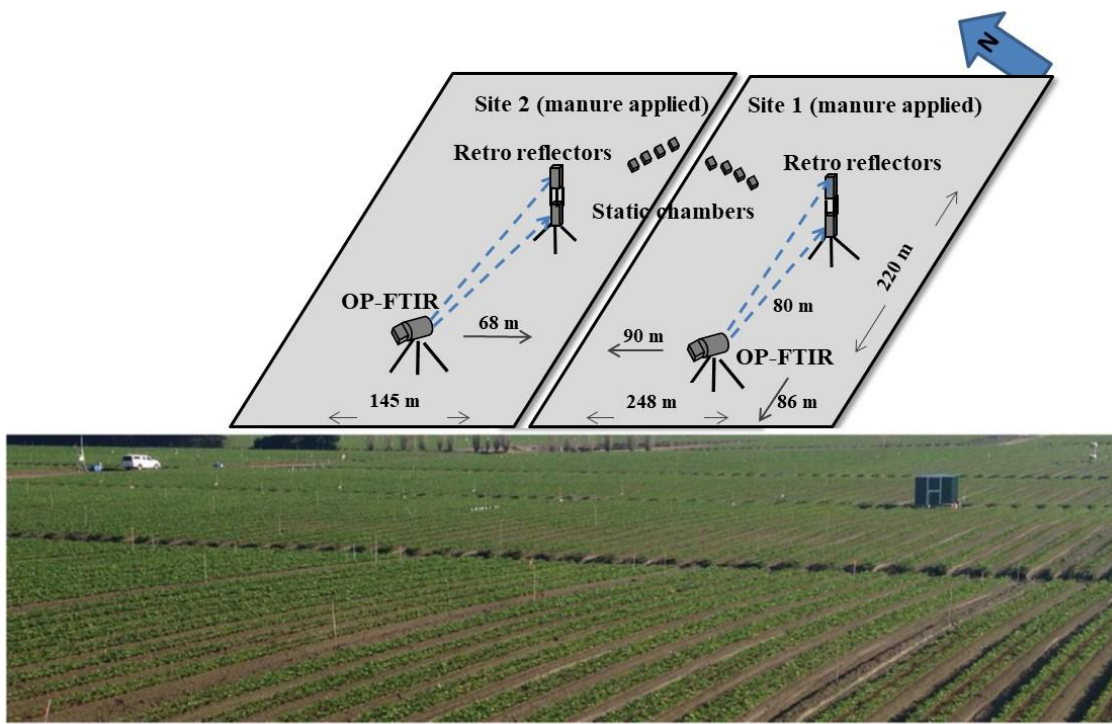
Figure 1 The design of the study (upper panel) and photo of experimental site with OP-FTIR set up (lower panel). Emission measurements were conducted with static chambers (four per site) and FG using the OP-FTIR spectroscopy system with retro reflectors at 0.8 and 1.8 m above ground. The figure is not in scale.

454

455

456

457

458

459   Figure 2

460

461
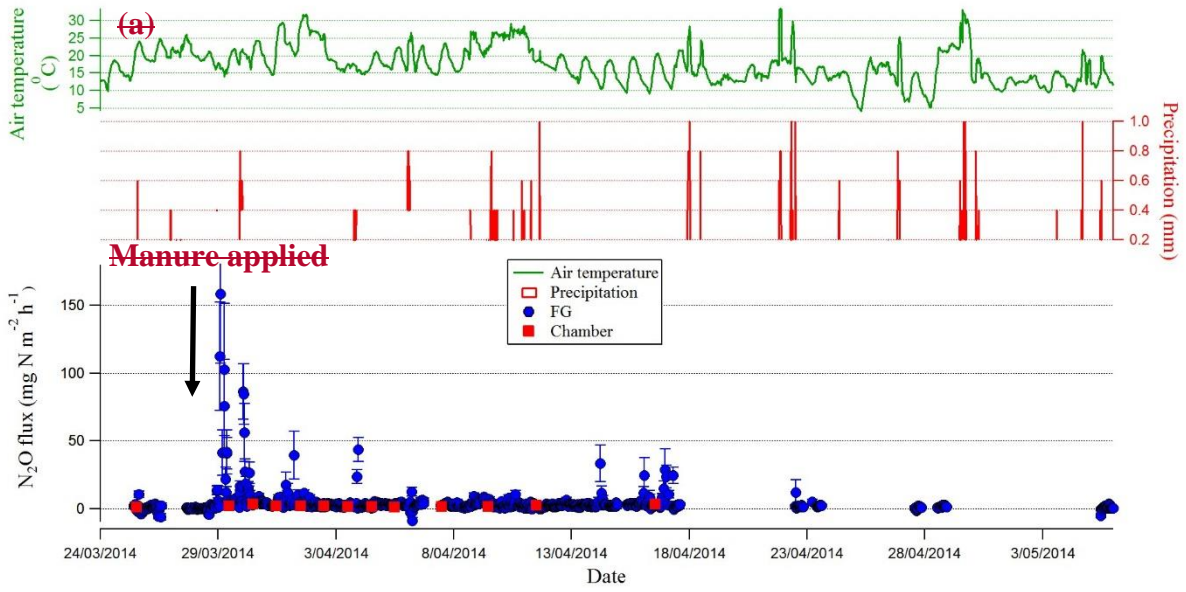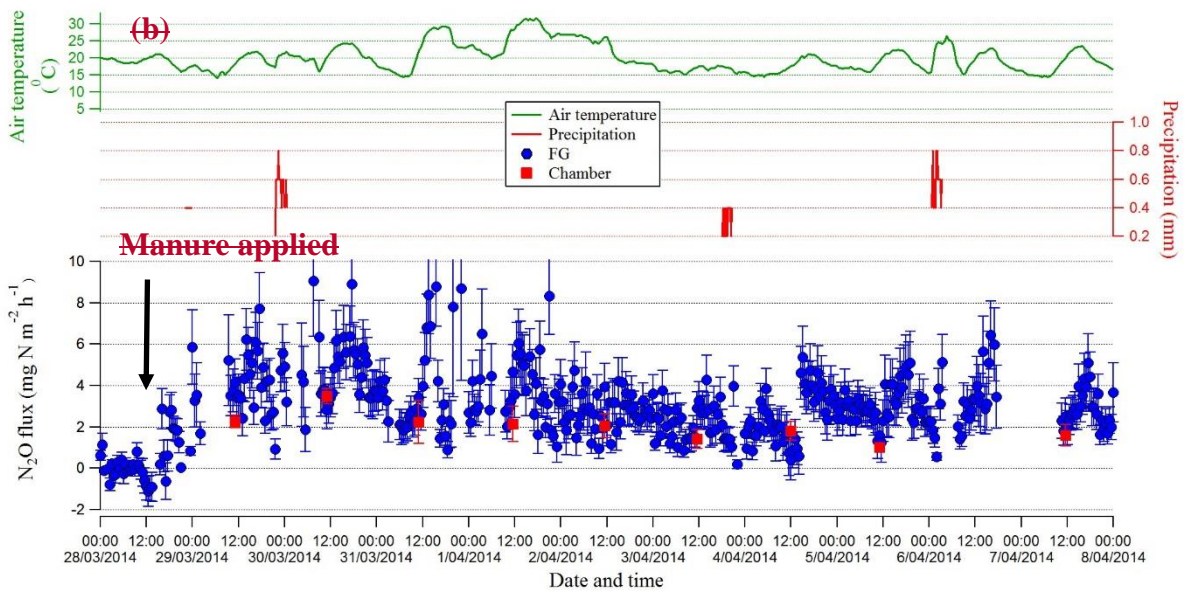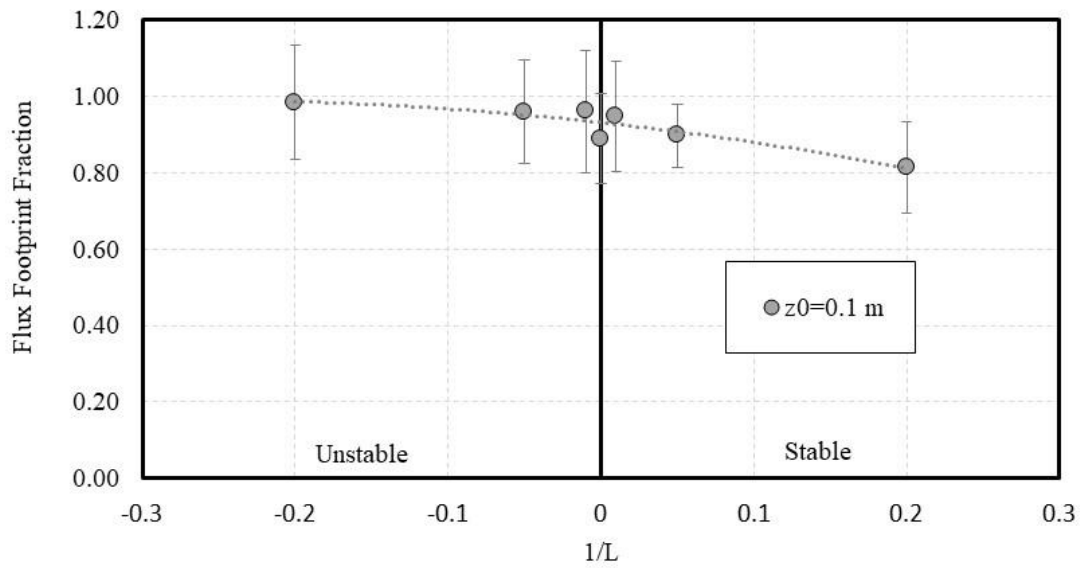
~~Figure~~ **2**

Figure 2 Estimated flux footprint fraction at Site 2, ploted versus atmospheric stability (the reciprocal of the Obukhov length *L*). The model results are for a roughness length $z_0 = 0.1$ m.

Figure 3

469
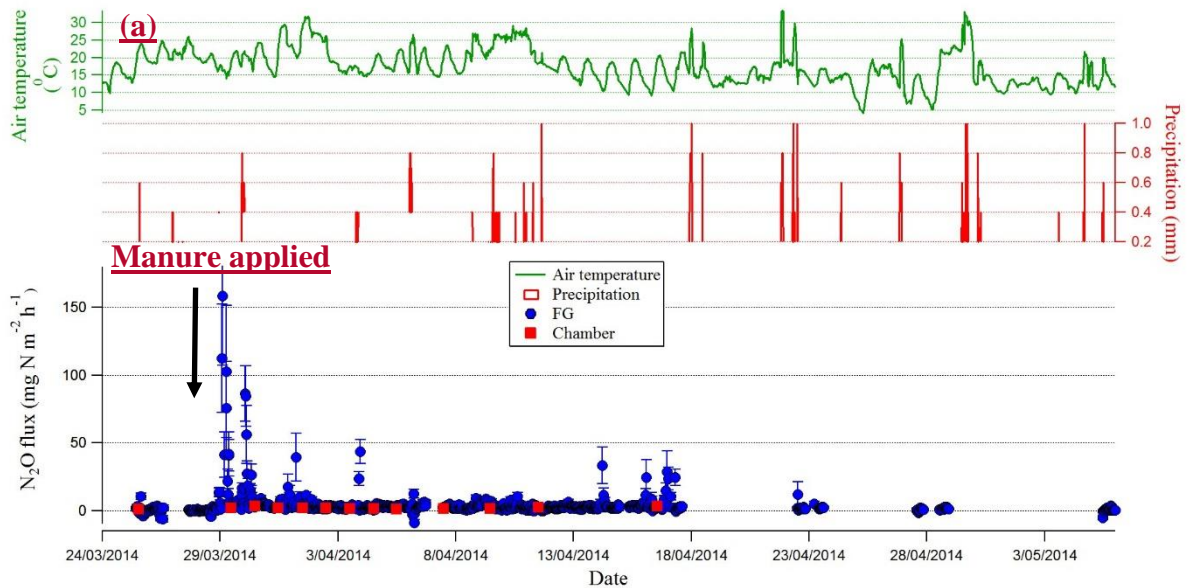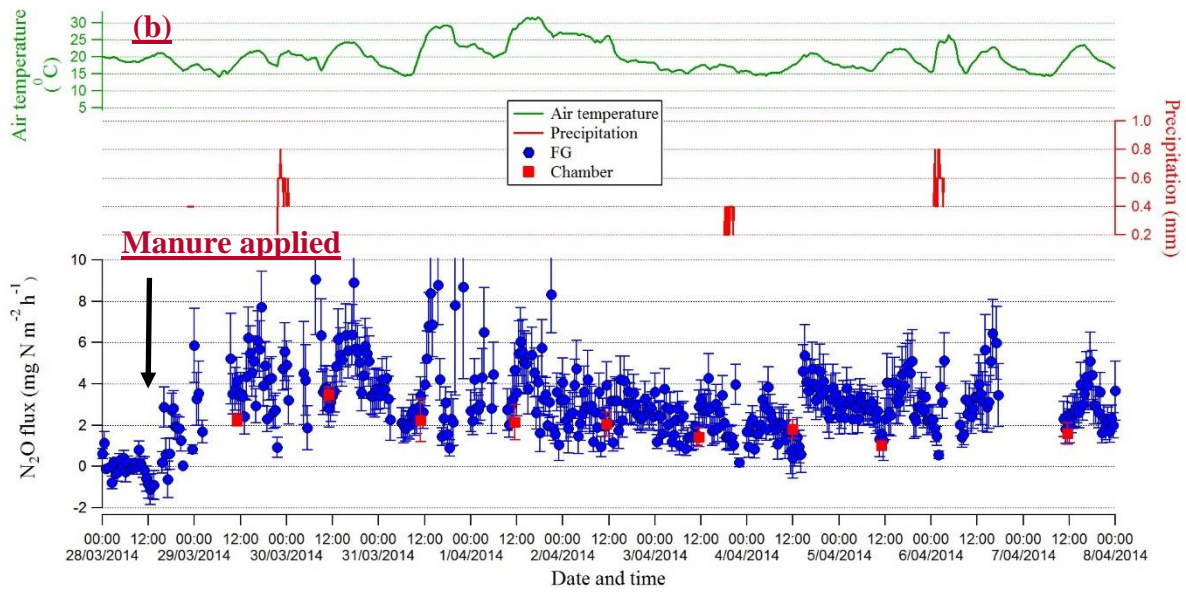
Figure 3 (a) Hourly N$_2$O fluxes measured by FG and static chambers from 25 March to 6 May. Air temperature and precipitation are plotted during the same period; and (b) subset of N$_2$O fluxes from 28 March to 8 April. Error bars (both upper and lower panels) represent 1−σ estimate of measurement uncertainty (δ_{QFG}) for the FG measurements and standard error for chambers. Manure was applied on 28 March 2014.

475

476

477

478

479

480

481

482

483

484

485

486

21

487   Anonymous refere#1

488   Re: Revision of manuscript Number: AMT-2018-90, Title: **Comparison of flux gradient and**
489   **chamber techniques to measure soil N$_2$O emissions**
490
491
492   We thank the positive feedback on the manuscript.

493   Reviewer is aware of the difference in N$_2$O fluxes between these two techniques that is mainly because
494   that the static chamber measurements were obtained periodically (no measurements during night-
495   time or morning). Reviewer suggested to compare the cumulative flux over the first 10 days after N
496   fertilizer was applied.

497   we agree, and the chamber vs. FG comparison was only evaluated during periods of concurrent
498   measurements. In the revised manuscript, we have summarised our footprint analysis on FG fluxes
499   and the investigation of the bias of chamber measurements using linear *dC/dt*.

500   The cumulative flux is often estimated by summing the mean daily flux over a period of time. Ideally,
501   a continuous real time series (or regular measurements during the day) should be used as emissions
502   can vary throughout the day. As we used chambers measurements only from 11 am to noon each day,
503   calculating   cumulative   fluxes   using   the   chamber   data   would   result   in   a   biased
504   estimation. Furthermore, a cumulative flux ratio between the two measurement methods would only
505   provide one data point, which would preclude inference.

506

507

508

509

510

511

512

513

514

515

516

517

518

519   Refere #2

520   Dear Dr. Flechard,

521   Re: Revision of manuscript Number: AMT-2018-90, Title: **Comparison of flux gradient and**
522   **chamber techniques to measure soil N_2O emissions**
523
524
525   We thank the positive feedback on the manuscript. We have addressed the comments thoroughly,
526   our response to every issue raised is given point by point in **blue text** below.

527
528
529   The reviewer is aware of the conclusions that should count two aspects: 1) quantitative footprint
530   analysis, 2) recalculate the chamber fluxes using non-linear algorithms.

531

532   Authors agree with the reviewer.

533   We conducted a footprint analysis using the Windtrax dispersion model to examine the contribution

534   of area outside our plot to the slant-path FG fluxes. We examined Site 2 (the smaller plot) and

535   considered a wind direction which would be the worst-case scenario for a footprint (wind from

536   NE). We also considered the atmospheric stability ($1/L$) and surface roughness (z_0). We estimated the

537   footprint of the slant-path configuration, and what fraction of the surface flux occurred within the plot

538   boundary. Figure A shows the Estimated flux footprint fraction at Site 2 increased from stable to

539   unstable conditions at z_0 = 0.1 m.
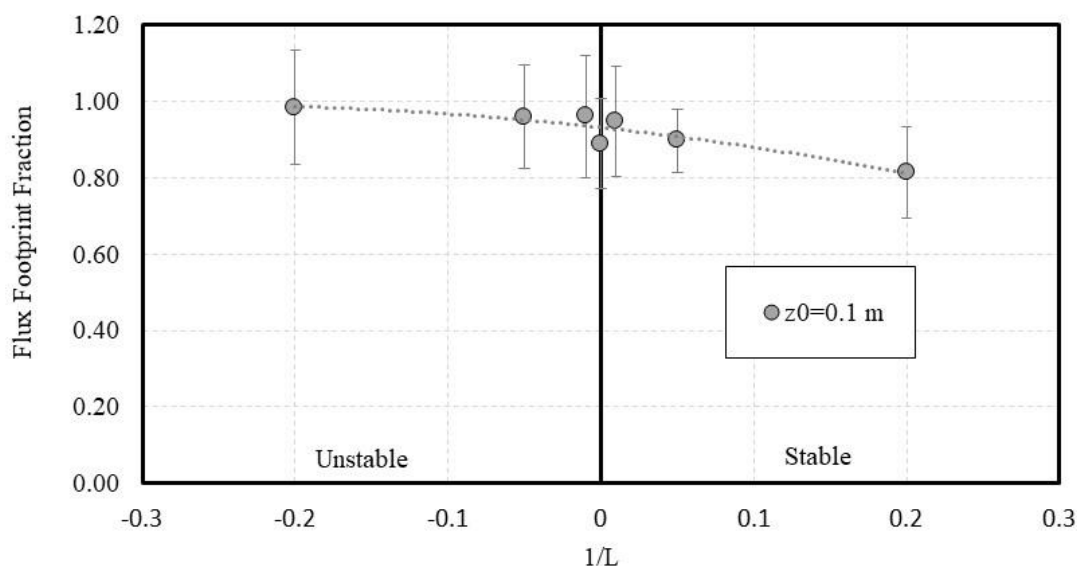
540

541   **Fig. A** Estimated flux footprint fraction at Site 2, plotted versus atmospheric stability (the reciprocal of

542   the Obukhov length L). The model results are for a roughness length z_0 = 0.1 m.

543   This result suggests the OP-FTIR flux estimates at night-time could be contaminated by emissions

544   outside the plot (up to 40% contaminated). However, the contamination decreases to < 10% during

545   the day time.

546

547   The results are summarised in the revised manuscript, see on page 7-8, Line 166-188 and Figure 2.

548   *"The FG flux measurements correspond to surface emissions within a flux "footprint". The footprint*

549   *generally extends upwind of the concentration sensors, but its spatial size varies with wind*

550   *conditions. A concern of this study is that the FG footprint extends beyond our plots, and the calculated*

551   *emission rates are "contaminated" by emissions occurring outside the plot. This possibility was*

552   *investigated by modelling the FG footprint for our smaller Site 2, where the contamination concerns*

553   *are greater. The WindTrax dispersion software (thunderbeachscientific.com) was used to simulate the*

554   *OP-FTIR slant-path setup, and calculate the fraction of the FG measured flux occurring within the Site*

555   *2 plot. We looked at the wind direction that results in a short fetch (NE), and looked at different*

556   *atmospheric stability conditions and roughness lengths. The results for z_0 = 0.1 m (representative of*

557   *the plot) are shown in Figure 2. We concluded that during stable night-time conditions the FG emission*

558   *calculations for Site 2 maybe contaminated by up to 40% by outside fluxes. This may result in either*

559   *over- or under-estimation of Site 2 emissions depending on the emission rate outside the plot. In*

560   *unstable daytime conditions the contamination potential falls to 0 – 10%. Contamination at Site 1 will*

561   *not be as serious due to the larger fetches.*

562   *The main objective of our study is to compare chamber and FG emission estimates. We looked at*

563   *periods with concurrent measurements from the two techniques, and hourly flux ratios of $Q_{FG}/Q_{chamber}$*

564   *measured between 10:00 and 13:00 are compared. Because the comparison took place during the day*

565   *when conditions were generally unstable, the FG contamination potential is low (and will be*

566   *ignored). The contamination potential does highlight a concern with micrometeorological*

567   *measurements, that a large measurement footprint may extend outside the study area and result in*

568   *measurement errors."*

569

570   2) For our chamber analysis we added an alternative estimation of the rate of *dC/dt,* using a non-linear

571   monomolecular model (Bolker, 2007). This follows the equation: $C_{N2O} = a_0 + a_1 (1 - \exp(-a_2/a_1 * t))$,

572   where C_{N2O} is the mole fraction of N_2O, a_0 is the intercept corresponding to N_2O mole fraction at time

573   *t* = 0, a_1 is the horizontal asymptote at t = +∞, a_2 is the slope (*dC/dt*) at *t* = 0, and *t* is time after the

574   chamber is chamber placement time (h).

575   We plotted dC/dt estimated from both the original linear regression and non-linear monomolecular

576   model in Figs. B, C. The chamber fluxes using the non-linear *dC/dt* estimate is 1.15 times higher than

577   that using linear *dC/dt* estimate. This improved the geometric mean $Q_{FG}/Q_{chamber\_non\text{-}linear}$ to 1.22

578   (confidence interval of 0.99 to 1.49). We still concluded that chamber measurements are

579   underestimating the flux, but the use of a non-linear calculation of *dC/dt* decreases the disagreement

580   to 22% compared to that of 40% using linear regression model.

581   We also added this discussion in the revised manuscript, see page 11-12, Line 269-284.

582   *"To examine the potential bias in N_2O emissions when dC/dt is estimated with a linear regression*

583   *model, we also calculated the results using a non-linear monomolecular model (Bolker, 2007). The*

584   *monomolecular model is one of the simplest saturating functions and follows (Eq. 4):*

585    $C_{N2O} = a_0 + a_1 (1 - exp(-a_2/a_1 * t))$ (4)

586   *where C_{N2O} is the mole fraction of N_2O, a_0 is the intercept corresponding to the N_2O mole fraction at*

587   *time t = 0, a_1 is the horizontal asymptote at t = +∞, a_2 is the slope (dC/dt) at t = 0, and t is time after*

588   *chamber placement (h).*

589

590   *Chamber fluxes calculated using the non-linear dC/dt ($Q_{chamber\text{-}non\text{-}linear}$) were 1.15 times higher than*

591   *$Q_{chamber}$ estimated using linear regression. Comparing the concurrent fluxes of Q_{FG} and $Q_{chamber\text{-}non\text{-}linear}$,*

592   *we found the geometric mean of $Q_{FG}/Q_{chamber\text{-}non\text{-}linear}$ to be 1.22 (confidence interval of 0.99 to 1.49).*

593   *Using 10,000 bootstrap re-samples (Efron and Tibshirani, 1994), we computed 10,000 potential mean*

594   *fluxes from the non-linear model, of which 9540 of the means were greater than 1, and 460 were lower*

595   *than 1. This result suggests the use of the non-linear dC/dt calculation has resulted in better agreement*

596   *with the FG estimates."*
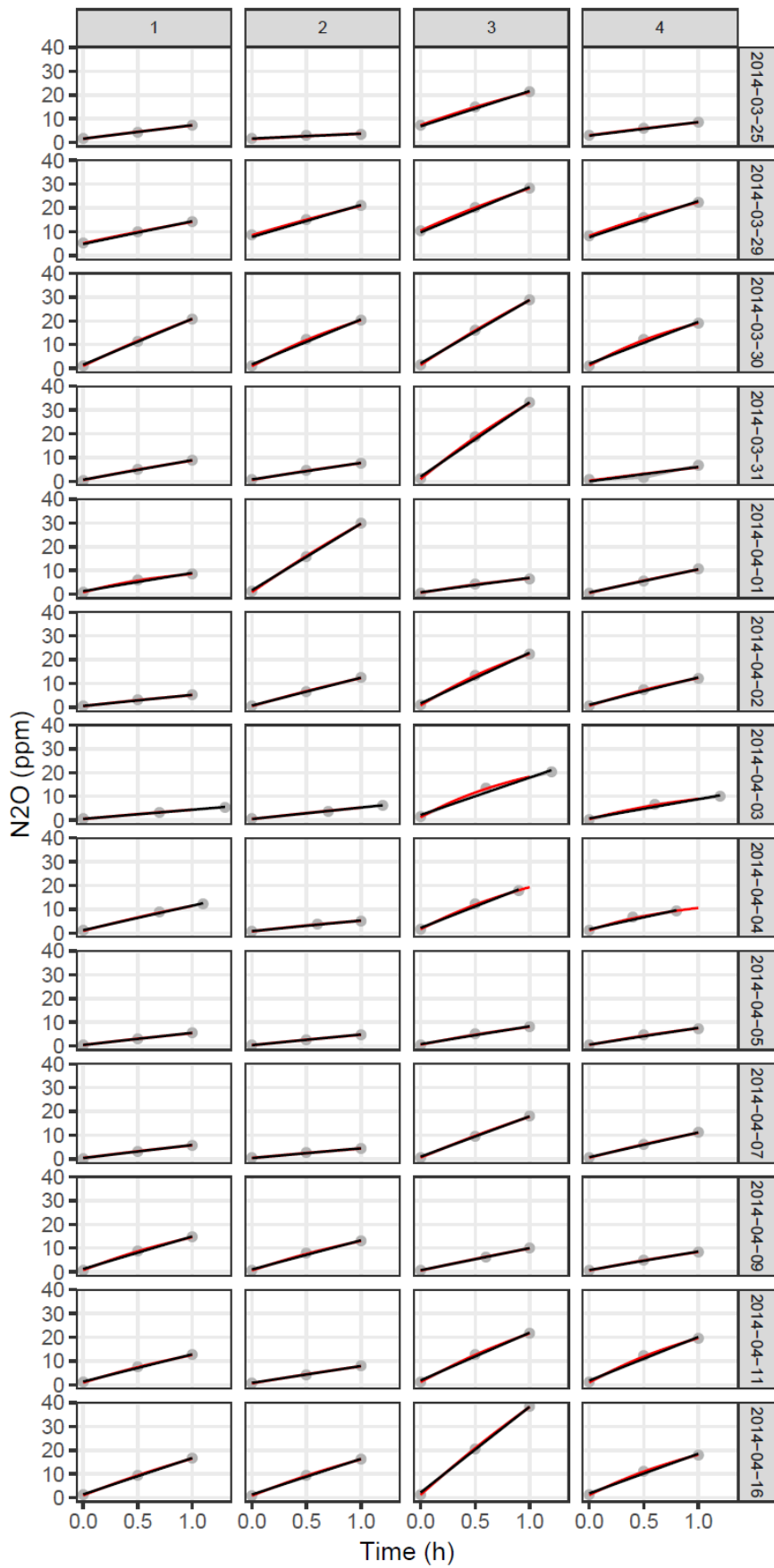
Fig. B. the N_2O concentration (ppm) changes with time (hour). The slope of the regression (dC/dt) using linear regression (black) and non-linear monomolecular model (red).

Special comments

Title. Agree with the reviewer, and the title has been changed.

P5, L109. We calculated the rate of dC/dt using a simple linear regression model. Following the reviewer's suggestion, we calculated the dC/dt using a non-linear monomolecular model.

We added couple of paragraphs in the revised manuscript, see page 11-12, Line 269-284. Refer to above text.

And Conclusions on page 12, Line 295-297.

" Our results showed that soil N_2O emissions measured by FG and static chambers (linear dC/dt) were statistically different, with fluxes from FG being on average 40% higher. Using a non-linear calculation of dC/dt in the chambers decreased the disagreement to 22%."

 P6, L140. We have provided the precisions on page 6, Line 144-145. "OP-FTIR system measures multiple gas concentrations (N_2O, CH_4, NH_3, CO_2, CO and water vapour) with high precision (N_2O < 0.3 ppb, CH_4 < 2 ppb, NH_3, 0.4ppb, CO_2, 1 ppm, CO, 0.1 ppb, and water vapour < 5%)."

P7, Line 170-171 and Fig.2. The background N_2O flux is about 0.6 mg $N_2O–N$ m^{-2} h^{-1} prior to manure application. In this study, the topsoil (0–15 cm) had high N contents: 52 mg $NH_4^+–N$ kg^{-1} and 118 mg $NO_3^-–N$ kg^{-1} before manure application. Therefore, the high background N_2O flux is reasonable.

P8, Line 192-193. We agree with the reviewer. We made the changes to be "agreement with the FG measurements in terms of the long-term background exchange patterns…". See page 9, Line 222.

P10. Line 237. As suggested, we calculated the chamber fluxes using the rate of dC/dt estimated using non-linear monomolecular model. The changes can be seen on page 11-12, Line 269-284, and Conclusions, Line 295-297.

P10, Line 247-248. We agree with the reviewer. As mentioned previously, we conducted a footprint analysis using Windtrax dispersion model, and added the results at page 7-8, Line 166-188 and Figure 2. We also removed the statement "In addition, concerns about FG arise if the fetch…occurring upwind of our sites." The changes can be seen on page 12, Line 286-288.

627 P 11, Line 249-250. The reviewer is correct. We have addressed this comment and added the footprint

628 analysis results on page 7-8, Line 166-188. Refer to the above text.

629

630 P11. Conclusion, Line 263-265. In the Conclusions, we added a sentence *"Our results showed that soil*

631 *N_2O emissions measured by FG and static chambers (linear dC/dt) were statistically different, with*

632 *fluxes from FG being on average 40% higher. Using a non-linear calculation of dC/dt in the chambers*

633 *decreased the disagreement to 22%."* see page 12, Line 295-297.

634 Our study supports the statement that chamber measurements underestimate the fluxes. See page

635 13, Line 301-303.

636 *"However, the relationship we observed, together with other reports on the biases created by chamber*

637 *calculation procedures, supports an interpretation that our FG emission calculations were accurate*

638 *and in this instance the chamber measurements were biased too low."*

639

640 **Technical Corrections**

641 P1. Abstract. Agree with the reviewer, the changes have been made.

642 P1, Line 12. Agree. Have added "aerodynamic" and removed "micrometeorological". See page 1, Line

643 13, and P3, Line 59.

644 P2, Line 42. Agree. "manually operated" has been added to "static chambers", see page 2, Line 43.

645 P2, Line 44. Agree. Change has been made to be" The temporal variation issue can be addressed by…",

646 see page 2, Line 45.

647 P3, Line 59-60. We agree with the reviewer. Change has been made to be" an estimate of the turbulent

648 diffusivity", see page 3, Line 61.

649 P4, Line 86. Agree with the reviewer. The sentence has been changed to be "The average daily

650 minimum and maximum temperature were 6 and 33°C, respectively." See page 4, Line 87.

651 P5, Eq. 1. Agree. We have modified the equation, see page 5, Line 107-113.
652
653 *"$Q_{chamber} = K_{N2O} (273/T) (V/A) dC/dt$* $\qquad\qquad\qquad\qquad\qquad\qquad$ *(1)*

654 *where $Q_{chamber}$ is the gas flux (μg N_2O–N m^{-2} h^{-1}); K_{N2O} is 1.25 (μg N μL^{-1}) according to the ideal gas law,*

655 *where K_{N2O} = P m/R T_0, and P is air pressure (at 1 atm), m is molecular mass (28 g mol^{-1}), R is gas*

656 *constant (0.0821 L atm K^{-1} mol^{-1}), and T_0 is 273 K; T is the air temperature within the chamber (K); V is*

657 *the total volume of headspace (L); A is a surface area inside the chamber (m^2); and dC/dt is the rate of*

658 *change in mole fraction of N_2O in the chamber ($\mu L\ L^{-1}\ h^{-1}$) determined by linear regression model. The*

659 *N_2O mole fraction is provide by GC, in ppm.*"

660 P6, Line 126. Because the path height is a function of x, when "kappa" is integrated with x, there is an

661 implicit integration with z. Therefore, there is no error in the formula and the statement.

662 P7, Line 153-154. Agree. The sentence has been modified as "…at a frequency of 10 Hz." See page 7,
663 Line 160.

664 P7, Line 155. Agree. The sentence has been changed to be "Atmospheric stability parameters of

665 friction velocity (u_*), surface roughness (z_0) and Obukhov stability length (L) were calculated from the

666 ultrasonic anemometer data." See page 7, Line 162-163.

667 P7, Line 168. We agree with the reviewer. The subtitle has been changed to be "The flux gradient

668 fluxes". See page 8, Line 197.

669 P9, Line 200. We agree with the reviewer. The subtitle has been changed to "Comparison of the two
670 measurement techniques". See page 10, Line 229.

671 P10, Line 235. We agree with the reviewer. The sentence has been changed to be "Several researchers

672 have reported that chamber flux calculation procedures introduced large uncertainty in N_2O

673 emissions.", see page 11, Line 264.

674

675

676 **References**

677 Abdi, D., Cade-Menun, B.J., Ziadi, N., Parent, L.-É., 2015. Compositional statistical analysis
678 of soil ^{31}P-NMR forms. Geoderma. 257–258, 40-47.

679 Anthony, W.H., Hutchinson, G.L., Livingston, G.P., 1995. Chamber measurement of soil-
680 atmosphere gas exchange: Linear vs. diffusion-based flux models. Soil Sci. Soc. Am. J. 59,
681 1308-1310.

682 Bai, M., 2010. Methane emissions from livestock measured by novel spectroscopic
683 techniques, School of Chemistry. University of Wollongong, p. 303.

684 Bolker, B., 2007. Ecological Models and Data in R. Princeton University Press, The United
685 States of America.

686 Christensen, S., Ambus, P., Arah, J.R.M., Clayton, H., Galle, B., Griffith, D.W.T.,
687 Hargreaves, K.J., Klemedtsson, L., Lind, A.M., Maag, M., Scott, A., Skiba, U., Smith, K.A.,
688 Welling, M., Wienhold, F.G., 1996. Nitrous oxide emission from an agricultural field:
689 comparison between measurements by flux chamber and micrometerological techniques.
690 Atmos. Environ. 30, 4183.

691   Dalal, R.C., Allen, D.E., Livesley, S.J., Richards, G., 2008. Magnitude and biophysical
692   regulators of methane emission and consumption in the Australian agricultural, forest, and
693   submerged landscapes: a review. Plant Soil. 309, 43-76.

694   de Klein, C.A.M., Sherlock, R.R., Cameron, K.C., van der Weerden, T.J., 2001. Nitrous
695   oxide emissions from agricultural soils in New Zealand—A review of current knowledge and
696   directions for future research. J. Roy. Soc. New Zeal. 31, 543-574.

697   Denmead, O.T., 1979. Chamber systems for measuring nitrous oxide emission from soils in
698   the field. Soil Sci. Soc. Am. J. 43, 89-95.

699   Denmead, O.T., 1995. Novel meteorological methods for measuing trace gas fluxes. Philos.
700   T. R. Soc. A. 351, 383-396.

701   Denmead, O.T., 2008. Approaches to measuring fluxes of methane and nitrous oxide between
702   landscapes and the atmosphere. Plant and Soil. 309, 5-24.

703   Denmead, O.T., Chen, D., Griffith, D.W.T., Loh, Z.M., Bai, M., Naylor, T., 2008. Emissions
704   of the indirect greenhouse gases NH_3 and NO_x from Australian beef cattle feedlots. Aust. J.
705   Exp. Agr. 48, 213-218.

706   Denmead, O.T., Macdonald, B.C.T., Bryant, G., Naylor, T., Wilson, S., Griffith, D.W.T.,
707   Wang, W.J., Salter, B., White, I., Moody, P.W., 2010. Emissions of methane and nitrous
708   oxide from Australian sugarcane soils. Agric. Forest Meteorol. 150, 748-756.

709   Efron, B., Tibshirani, R.J., 1994. An intruduction to bookstrap. Chapman&Hall/CRC, Boca
710   Raton, London, New York, Washington, D.C.

711   Flesch, K.T., Baron, V., Wilson, J., Griffith, D.W.T., Basarab, J., Carlson, P., 2016.
712   Agricultural gas emissions during the spring thaw: Applying a new measuremnt technique.
713   Agric. Forest Meteorol. 221, 111-121.

714   Flesch, T.K., McGinn, S.M., Chen, D.L., Wilson, J.D., Desjardins, R.L., 2014. Data filtering
715   for inverse dispersion emission calculations. Agric. Forest Meteorol. 198-199, 1-6.

716   Flesch, T.K., Prueger, J.H., Hatfield, J.L., 2002. Turbulent Schmidt number from a tracer
717   experiment. J. Appl. Meteorol. 111, 299-307.

718   Griffith, D.W.T., 1996. Synthetic calibration and quantitative analysis of gas-phase FT-IR
719   spectra. Appl. Spectrosc. 50, 59-70.

720   Griffith, D.W.T., Bryant, G.R., Hsu, D., Reisinger, A.R., 2008. Methane emissions from free-
721   ranging cattle: comparison of tracer and integrated horizontal flux techniques. J. Environ.
722   Qual. 37, 582-591.

723   Griffith, D.W.T., Deutscher, N.M., Caldow, C., Kettlewell, G., Riggenbach, M., Hammer, S.,
724   2012. A Fourier transform infrared trace gas and isotope analyser for atmospheric
725   applications. Atmos. Meas. Tech. 5, 2481-2498.

726   Griffith, D.W.T., Galle, B., 2000. Flux measurements of NH_3, N_2O and CO_2 using dual beam
727   FTIR spectroscopy and the flux gradient technique. Atmos. Environ. 34, 1087-1098.

728 Hargreaves, K.J., Wienhold, F.G., Klemedtsson, L., Arah, J.R.M., Beverland, I.J., Fowler, D.,
729 Galle, B., Griffith, D.W.T., Skiba, U., Smith, K.A., Welling, M., Harrris, G.W., 1996.
730 Measurement of nitrous oxide from Agricultural land using micrometeorological methods.
731 Atmos. Environ. 30, 1563-1571.

732 Hutchinson, G.L., Mosier, A.R., 1981. Improved soil cover method for field measurement of
733 nitrous oxide fluxes. Soil Sci. Soc. Am. J. 45, 311-316.

734 Jones, S.K., Famulari, D., Di Marco, C.F., Nemitz, E., Skiba, U.M., Rees, R.M., Sutton,
735 M.A., 2011. Nitrous oxide emissions from managed grassland: a comparison of eddy
736 covariance and static chamber measurements. Atmos. Meas. Tech. 4, 2179-2194.

737 Judd, M.J., Kellier, F.M., Ulyatt, M.J., Lassey, K.R., Tate, K.R., Shelton, D., Harvey, M.J.,
738 Walker, C.F., 1999. Net methane emissions from grazing sheep. Global Change Biol. 5, 647-
739 657.

740 Laubach, J., Kelliher, F.M., 2004. Measuring methane emission rates of a dairy cow herd by
741 two micrometeorological techniques. Agric. Forest Meteorol. 125, 279-303.

742 Levy, P.E., Gray, A., Leeson, S.R., Gaiawyn, J., Kelly, M.P.C., Cooper, M.D.A., Dinsmore,
743 K.J., Jones, S.K., Sheppard, L.J., 2011. Quantification of uncertainty in trace gas fluxes
744 measured by the static chamber method. Eur. J. Soil Sci. 62, 811-821.

745 Li, J., Tong, X., Yu, Q., Dong, Y., Peng, C., 2008. Micrometeorological measurements of
746 nitrous oxide exchange above a cropland. Atmos. Environ. 42, 6992-7001.

747 Matthias, A.D., Yarger, D.N., Weinback, R.S., 1978. A numerical evaluation of chamber
748 methods for determining gas fluxes. Geophys. Res. Lett. 5, 765-768.

749 Neftel, A., Ammanna, C., Fischer, C., Spirig, C., Conen, F., Emmenegger, L., Tuzson, B.,
750 Wahlen, S., 2010. N_2O exchange over managed grassland: Application of a quantum cascade
751 laser spectrometer for micrometeorological flux measurements. Agric. Forest Meteorol. 150,
752 775-785.

753 Norman, J.M., Kucharik, C.J., Gower, S.T., Baldocchi, D.D., Crill, P.M., Rayment, M.,
754 Savage, K., Striegl, R.G., 1997. A comparison of six methods for measuring soil-surface
755 carbon dioxide fluxes. J. Geophys. Res. 102, 28771-28777.

756 Pattey, E., Strachan, I.B., Desjardins, R.L., Edwards, G.C., Dow, D., MacPherson, J.I., 2006.
757 Application of a tunable diode laser to the measurement of CH_4 and N_2O fluxes from field to
758 landscape scale using several micrometeorological techniques. Agric. Forest Meteorol. 136,
759 222-236.

760 Ruser, R., Flessa, H., Schilling, R., Steindl, H., Beese, F., 1998. Soil compaction and
761 fertilization effects on nitrous oxide and methane fluxes in potato fields. Soil Sci. Soc. Am. J.
762 62, 1587-1595.

763 Sommer, S.G., McGinn, S.M., Hao, X., Larney, F.J., 2004. Techniques for measuring gas
764 emissions from a composting stock pile of cattle manure. Atmos. Environ. 38, 4643-4652.

765 Turner, D.A., Chen, D., Galbally, I.E., Leuning, R., Edis, R.B., Li, Y., Kelly, K., Phillips, F.,
766 2008. Spatial variability of nitrous oxide emissions from an Australian irrigated dairy pasture.
767 Plant and Soil. 309, 77-88.

768 Venterea, R.T., 2013. Theoretical comparison of advanced methods for calculating nitrous
769 oxide fluxes using non-steady state chambers. Soil Sci. Soc. Am. J. 77, 709-720.

770 Venterea, R.T., Dolan, M., Ochsner, T.E., 2010. Urea decreases nitrous oxide emissions
771 compared with anhydrous ammonia in a Minnesota corn cropping system. Soil Sci. Soc. Am.
772 J. 74, 407-418.

773 Wang, K., Zheng, X., Pihlatie, M., Vesala, T., Liu, C., Haapanala, S., Mammarella, I.,
774 Rannik, Ü., Liu, H., 2013. Comparison between static chamber and tunable diode laser-based
775 eddy covariance techniques for measuring nitrous oxide fluxes from a cotton field. Agric.
776 Forest Meteorol. 171–172, 9-19.

777 Webb, E.K., Pearman, G.I., Leuning, R., 1980. Correction of flux measurements for
778 chemistry effects due to heat and water vapour transfer. Quart. J. R. Meteorol. Soc. 106, 85-
779 100.

780 Wilson, J.D., Flesch, T.K., 2016. Generalized flux-gradient technique pairing line-average
781 concentrations on vertically separated paths. Agric. Forest Meteorol. 220, 170-176.

782 Yao, Z., Zheng, X., Xie, B., Liu, C., Mei, B., Dong, H., Butterbach-Bahl, K., Zhu, J., 2009.
783 Comparison of manual and automated chambers for field measurements of N_2O, CH_4, CO_2
784 fluxes from cultivated land. Atmos. Environ. 43, 1888-1896.

785

786

787

788

789

790

791